



## BASIC SCIENCE ARTICLE

# CX3CR1 as a respiratory syncytial virus receptor in pediatric human lung

Christopher S. Anderson<sup>1,2</sup>, Chin-Yi Chu<sup>1,2</sup>, Qian Wang<sup>1,2</sup>, Jared A. Mereness<sup>1,2</sup>, Yue Ren<sup>1,2</sup>, Kathy Donlon<sup>1,2</sup>, Soumyaroop Bhattacharya<sup>1,2</sup>, Ravi S. Misra<sup>1</sup>, Edward E. Walsh<sup>3,4</sup>, Gloria S. Pryhuber<sup>1</sup> and Thomas J. Mariani<sup>1,2</sup>

**BACKGROUND:** Data on the host factors that contribute to infection of young children by respiratory syncytial virus (RSV) are limited. The human chemokine receptor, CX3CR1, has recently been implicated as an RSV receptor. Here we evaluate a role for CX3CR1 in pediatric lung RSV infections.

**METHODS:** CX3CR1 transcript levels in the upper and lower pediatric airways were assessed. Tissue localization and cell-specific expression was confirmed using *in situ* hybridization and immunohistochemistry. The role of CX3CR1 in RSV infection was also investigated using a novel physiological model of pediatric epithelial cells.

**RESULTS:** Low levels of CX3CR1 transcript were often, but not always, expressed in both upper (62%) and lower airways (36%) of pediatric subjects. CX3CR1 transcript and protein expression was detected in epithelial cells of normal human pediatric lung tissues. CX3CR1 expression was readily detected on primary cultures of differentiated pediatric/infant human lung epithelial cells. RSV demonstrated preferential infection of CX3CR1-positive cells, and blocking CX3CR1/RSV interaction significantly decreased viral load.

**CONCLUSION:** CX3CR1 is present in the airways of pediatric subjects where it may serve as a receptor for RSV infection. Furthermore, CX3CR1 appears to play a mechanistic role in mediating viral infection of pediatric airway epithelial cells *in vitro*.

*Pediatric Research* (2020) 87:862–867; <https://doi.org/10.1038/s41390-019-0677-0>

## INTRODUCTION

Almost all children are infected with respiratory syncytial virus (RSV) during their first 2 years of life. RSV infection typically originates in the upper airways of young children and can be found in the lower airways during severe cases. RSV replication in the airways occurs primarily in epithelial cells and these cells are readily infected *in vitro*. The innate host properties that make epithelial cells prone to RSV infection are still not well understood.<sup>1,2</sup>

To date, there is no consensus on a specific host receptor that RSV uses for attachment to the host epithelium to initiate infection. Studies of RSV attachment have demonstrated that addition of heparin, heparan sulfate, or chondroitin to submerged cell lines significantly decreases RSV–cell association.<sup>3</sup> Other studies have shown that this interaction was specific to particular heparan sulfate and chondroitin molecules.<sup>1</sup> These findings have been complicated by contradictory results of studies of heparan sulfate proteoglycans expression on the lung epithelium, with some reporting the lack of expression or basal only expression and others noting expression on normal human bronchial epithelial cells grown *in vitro*.<sup>4–7</sup>

The fractalkine receptor, CX3CR1, is a 7-transmembrane G protein-coupled receptor known to be expressed in natural killer cells, cytotoxic CD8 T cells, monocytes, and dendritic cells. The CX3CR1 ligand, CX3CL1 (fractalkine), contains a CX3C motif and can be expressed on the cellular membrane or as a soluble form.

Fractalkine is expressed in the lung and is thought to play a role in migration and retention of immune cells in the tissue.<sup>8</sup> The presence of a CX3C motif on the RSV G protein has led to interest in the involvement of CX3CR1 in RSV infection.<sup>9–13</sup> RSV infection of *in vitro* models of preadolescent and adult epithelium have shown at least partial dependence upon CX3CR1/G protein binding.<sup>14,15</sup> Structural investigations have also demonstrated binding of G protein to CX3CR1. RSV replication has been shown to occur in ciliated cells in animal models,<sup>16</sup> and CX3CR1 and cilia have been shown to co-localize in adult epithelial cells *in vitro*.<sup>17</sup> RSV strains containing a CX3C to CX4C motif mutation show reduced replication *in vitro*.<sup>14</sup> Furthermore, prophylactic treatment with monoclonal antibodies targeting the CX3C motif has been shown to reduce RSV disease in mice.<sup>18,19</sup> Taken together, the CX3C motif of the RSV G protein is emerging as a CX3CR1 ligand that impacts infection by RSV.

Despite the clinical significance of RSV infection in children, no definitive studies have assessed the importance of CX3CR1 in pediatric RSV infection. Moreover, the extent of CX3CR1 expression in pediatric airways in humans is unclear. Using our unique access to normal newborn and pediatric human lung tissues, as well as our newly developed pediatric lung epithelial cell model, we set out to examine the expression of CX3CR1 in the pediatric lung and test its role in RSV infection of pediatric airways.

<sup>1</sup>Division of Neonatology, Department of Pediatrics, University of Rochester Medical Center, Rochester, NY, USA; <sup>2</sup>Program in Pediatric Molecular and Personalized Medicine, Department of Pediatrics, University of Rochester Medical Center, Rochester, NY, USA; <sup>3</sup>Department of Medicine, University of Rochester Medical Center, Rochester, NY, USA and <sup>4</sup>Department of Medicine, Rochester General Hospital, Rochester, NY, USA  
Correspondence: Thomas J. Mariani (Tom\_Mariani@urmc.rochester.edu)

Received: 7 August 2019 Revised: 22 October 2019 Accepted: 2 November 2019  
Published online: 14 November 2019

## METHODS

### Virus propagation

The green fluorescent protein (GFP) containing RSV (A2 strain)<sup>10</sup> was grown in HEp-2 cells as previously described.<sup>20</sup> Cells were incubated with virus at 37 °C for 2 h, supernatant removed, and 5 ml of virus medium (2% fetal bovine serum (FBS) Minimal Essential Medium) was added to the flask. Virus was allowed to propagate for 5–7 days until cytopathic effect was observed. Virus containing supernatant was aspirated and centrifuged at 300 × *g* for 10 min to remove cell debris. Cleared supernatant was aliquoted into cryopreserved vials. Vials were immediately flash frozen in liquid nitrogen and stored at –80 °C until usage.

### Virus focus-forming unit (FFU) quantification

To quantify virus plaque-forming units (FFU), HEp-2 cells were seeded onto 96-well plates (Costar 3596) at a density of  $2.5 \times 10^4$  cells per well in 200 µl of HEp-2 media ( $2.5 \times 10^6$  per 100 wells in 20 ml). The next day, 0.6% agarose (Sigma) in molecular-grade H<sub>2</sub>O was heated in a microwave until it melted (approximately 2 min) and placed in 42 °C water bath. Next, virus containing supernatant was quickly thawed at 37 °C in a water bath and a 10-fold dilution series was performed resulting in 11 dilutions. Cells were subsequently washed with Dulbecco's phosphate-buffered saline (DPBS) (+Ca+Mg). Virus (100 µl at each dilution) was added to wells in duplicate. In addition, 100 µl of virus media was used as a negative control. Inoculated cells were incubated at 37 °C for 1 h and rocked every 15 min to keep the culture covered and wet. After the 1-h incubation, virus supernatant was carefully removed. Heated (42 °C) agarose was diluted with HEp-2 growth medium at a ratio of 1:1 and quickly overlaid on top of the cells. Cultures were maintained at room temperature (RT) for 10 min to allow agarose to solidify. Cultures were incubated for 7 days at 37 °C. Viral concentrations were quantified using fluorescent microscopy and counted to determine the number of FFUs per ml (FFU/ml).

### Primary pediatric human epithelial cell model

Pediatric human lung epithelial (PHLE) cells were prepared as previously described.<sup>21</sup> Briefly, fresh donor-quality infant/pediatric lung tissues were digested with a protease cocktail containing collagenase type A (2 mg/ml), dispase II (1 mg/ml), elastase (0.5 mg/ml), and DNAase (2 mg/ml).<sup>22</sup> Single-cell suspensions were transferred to a T75 flask containing SAGM (Lonza) supplemented with 1% FBS. After 24 h, non-adherent cells were removed. Fibroblast-like cells were removed periodically by treatment with 0.0125% trypsin containing 45 µM EDTA in DPBS at RT. Once cells were 60–70% confluent, cells were trypsinized and 100,000 cells were seeded on rat tail collagen-I (34.5 µg/ml) coated Transwell inserts (12-well PET membrane, 0.4 µm pore size, 12 mm diameter). After 24 h, culture medium was changed to 1:1 mixture of BEBM (Lonza)/Dulbecco's modified Eagle's medium. After confluence (10–15 days), transepithelial electrical resistance was measured daily until resistance reached  $\geq 200$  Ohms-cm<sup>2</sup>, a sign of tight-junction formation. The apical medium was removed and cells were maintained at air-liquid interface (ALI). After transition to ALI, cells were maintained in PneumaCult-ALI medium containing supplements and hydrocortisone, according to manufacturer's instructions. ALI cultures were differentiated for 12–14 days at ALI.

### Virus infection

Differentiated (12–14 day ALI) PHLE cell cultures were infected via the apical surface with RSV (multiplicity of infection of 0.5–1) and incubated for 2 h at 37 °C. Virus were removed, cells were washed with PBS, and returned to the incubator for up to 48 h. For CX3CR1 antibody-blocking experiments, anti-CX3CR1 antibody (MBL- Cat# D070–3) was preincubated with PHLE cell cultures for 1 h at 37 °C prior to challenge with the virus. For purified recombinant CX3CR1 protein-blocking experiments, recombinant CX3CR1 was purchased

from Abnova (cat# H00001524-P01) and incubated with the virus for 1 h at 37 °C prior to virus challenge.

### Immunohistochemistry

Formalin-fixed paraffin-embedded (FFPE) lung tissues were obtained from the Human Tissue Core of the Developing Lung Molecular Atlas Program (LungMAP HTC). Tissue was deparaffinization by washing slides sequentially twice in Xylene, a 1:1 mixture of 100% ethanol/Xylene once, twice with 100% ethanol, once with 95% ethanol, once with 70% ethanol, once with 50% ethanol, each for 3 min, and finally rinsed with cold tap water. For antigen retrieval, slides were placed in an open vessel inside a vegetable steamer and covered with boiling sodium citrate buffer (10 mM sodium citrate, 0.05% Tween 20, pH 6.0) for 20 min. Slides were rinsed with running cold tap water for 10 min and washed twice for 5 min in Tris-buffered saline (TBS) containing 0.025% Triton X-100 with gentle agitation and subsequently blocked in 10% normal goat serum with 1% bovine serum albumin (BSA) in TBS for 2 h at RT. Slides were drained and excess liquid removed. Rabbit anti-CX3CR1 antibody (Abcam ab8021) was diluted 1:50 in TBS with 1% BSA and mixed with mouse anti-acetylated tubulin diluted 1:100. Two hundred microliters of diluted antibody mixture was added to each slide and incubated overnight at 4 °C. Normal mouse immunoglobulin G (IgG) and goat IgG served as negative controls. After overnight incubation, slides were rinsed twice for 5 min with TBS with 0.025% Triton, with gentle agitation. Fluorophore-conjugated anti-mouse and anti-rabbit secondary antibody was diluted 1:1000 in TBS with 1% BSA. Two hundred microliters of diluted secondary antibody mixture was added to each slide and incubated for 1 h at RT in the dark. After incubation, slides were rinsed three times for 5 min with TBS. Slides were mounted using ProLong Gold Antifade mounting medium (Life Technologies). Slides were incubated overnight at RT to allow slides to cure. Images were taken by first locating pseudostratified columnar structured cells on the section using bright field, then taking images with fluorescent filters. Immunohistochemistry was performed and images were taken on four subjects with three slides per subject.

### Fluorescent in situ hybridization (FISH)

FISH was performed using RNAscope technology (ACDbio), essentially according to the manufacturer's instructions. In brief, FFPE lung tissues were deparaffinized, target retrieved, and probed with CX3CR1 (ACDbio cat# 411251), FOXJ1 (ACDbio cat# 430921-C2), or SCGB1A1 (ACDbio cat# 469971-C3) transcript-specific probes using the RNAscope Multiplex Fluorescent Kit v2 (ACDbio cat# 323100) and Opal Fluorophores (PerkinElmer Opal 520, Opal 570, Opal 690, respectively). FISH was performed and images were taken on three subjects with two slides per subject.

### RNA quantification

Preinfection PHLE cell cultures derived from four subjects were used for CX3CR1 RNA quantification and postinfection PHLE cell cultures were used for RSV-M protein quantification. PHLE cell cultures were washed twice with PBS. Cells were lysed with 150 µl of RNA lysis buffer (Agilent) and RNA was extracted using the Absolutely RNA Micoprep Kit (Agilent) according to the manufacturer's protocol, including DNase treatment. RNA was quantified by Nanodrop spectrometry and 500 µg of RNA was used for cDNA synthesis (iScript; BIO-RAD). cDNA was diluted 1:20 with molecular-grade H<sub>2</sub>O and 6 µl of cDNA was added to 4 µl Power SYBR green PCR Master Mix (Applied Biosystems) containing Human CX3CR1 (FWD: AGTGTACCGACATTTACCTCC, REV: AAGG CGGTAGTGAATTTGCAC) or RSV-M protein (FWD: GGCAAATATGG AACATAGCTGAA, REV: TCTTTTCTAGGACATTGTATTGA ACAG) primers. Quantitative PCR was performed using Vii7 (Applied Biosystems).

**CX3CR1 protein quantification**

Preinfection differentiated PHLE cell cultures were washed with PBS and lysed with 50 µl RIPA buffer containing protease inhibitors (Thermo Scientific) for 5 min on ice. Lysates were spun at 10,000 ×g for 10 min and the supernatant was collected. CX3CR1 protein levels were determined by Sandwich-ELISA (myBioSource, MBS2505819) following the manufacturer's instructions.

**Flow cytometry**

Following RSV infection, cells were recovered by trypsinization (0.25%), blocked with BSA, and incubated with anti-CX3CR1 antibody (Abcam ab8021) for 1 h at RT. Cells were analyzed for GFP and CX3CR1 on a BD LSRII. Data were analyzed using the FlowJo Software.

**Statistics**

Statistics were performed using the R software base package. Significance was achieved using a *p* value of 0.05 threshold.

**RESULTS**

We interrogated CX3CR1 expression in an RNAseq database we have recently generated, describing upper airway gene expression in nasal swabs obtained from infants at ~1 month of age.<sup>23</sup> CX3CR1 transcript levels were detected in 33 out of 53 (62%) infant upper airway samples. CX3CR1 transcript levels varied between subjects ranging from 0.29 to 22.3 reads per million (RPM) normalized counts in subjects with detected CX3CR1 transcript (Fig. 1a). Among the 23,132 gene transcripts detected in any subject, mean CX3CR1 transcript level was >44% of the expressed genes. Among chemokine receptors, CX3CR1 transcript ranked 9 out of 19 (47%; Fig. 1b). Taken together, CX3CR1 transcript was detected in the majority of subjects, but not all, and the absolute expression levels varied widely.

We also interrogated CX3CR1 expression in a second database describing lower airway gene expression from 5 cell populations obtained from total tissue digests of infant/pediatric human lung lobes from LungMAP<sup>22</sup>: sorted epithelial (EPI; EPCAM+/CD45-), sorted endothelial (END; CD45-/CD31+), sorted mesenchymal cells (MES; CD45-/EPCAM-/CD31-), sorted mixed immune cells (MIC; CD45+), unsorted mixed pulmonary (PMX; unsorted), as well as tissues biopsies (BPS). CX3CR1 transcript was detected in all sample types (Fig. 1c). The highest CX3CR1 expression was found in mixed immune cells, followed by biopsy and mesenchymal. CX3CR1 transcript in sorted epithelial cells was detected in 4 out of 11 (36%) subjects, and when present, transcript counts were relatively low (1–6 RPM normalized counts). Taken together, CX3CR1 transcript was sometimes detected in lower respiratory tract epithelial cells from the pediatric lungs.

CX3CR1 expression in the pediatric lungs was also assessed in fixed lung tissues. FISH of histological sections from normal pediatric lungs detected CX3CR1 transcript in epithelial cells lining the airway, including those expressing FOXJ1, a ciliated cell differentiation maker (Fig. 2a). FISH identifies RNA transcripts primarily in the cytosol due to its short half-life in the nucleus. We found both co-fluorescence of CX3CR1 and FOXJ1 probes although co-fluorescence was not absolute. Immunohistochemistry for CX3CR1 protein also detected expression in airway epithelial cell (Fig. 2b), where CX3CR1 co-localized with acetylated tubulin, consistent with in vitro studies in adults.<sup>17</sup> Taken together, CX3CR1 transcript and protein is detectable in epithelial cells lining the airway of intact pediatric lung tissues.

Next, we assessed the expression of CX3CR1 in primary cultures of PHLE cell culture. PHLE cell cultures were differentiated at ALI in vitro, as previously described,<sup>21</sup> and compared to HEp-2 cells grown under standard submerged conditions. We found that CX3CR1 mRNA was consistently detected in both HEp-2 and PHLE cell cultures, with PHLE cell cultures expressing nearly fivefold greater levels (Fig. 3a). CX3CR1 transcript levels varied somewhat

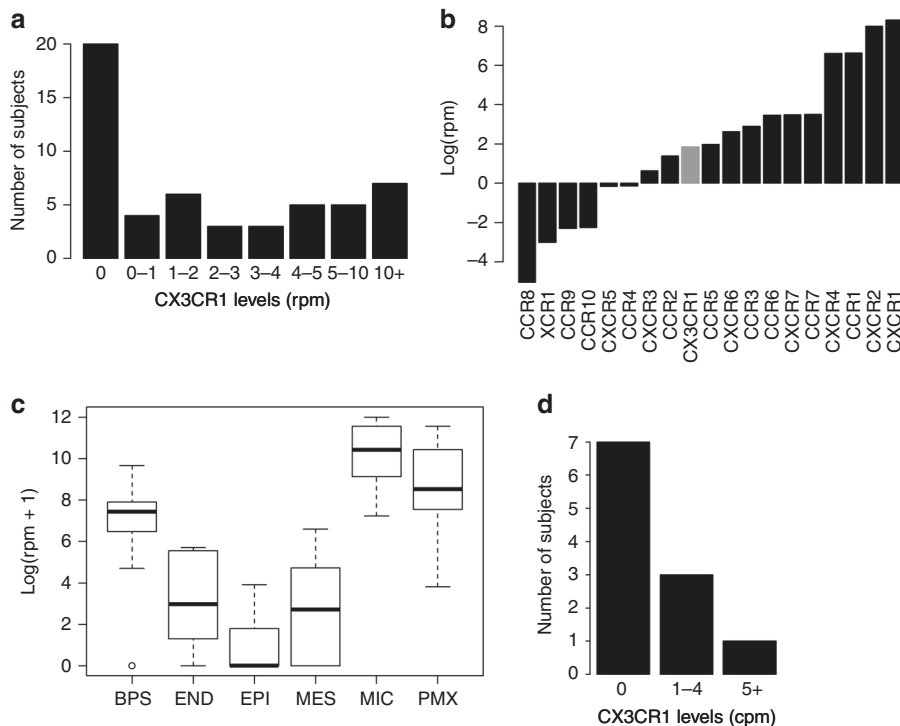


**Fig. 1** Pediatric airway CX3CR1 transcript levels. **a** CX3CR1 (reads per million (RPM)) transcript levels from RNA extracted from nasal swabs of young children (*N* = 53). **b** Chemokine receptor transcript levels of RNA extracted from nasal swabs of young children (*N* = 53). **c** CX3CR1 gene expression from cells sorted after lung digest (BPS biopsy, END endothelial, EPI epithelial, MES mesenchymal, MIC mixed immune cells, PMX mixed pulmonary) (*N* = 11). **d** CX3CR1 transcript levels of sorted epithelial cells population (*N* = 11).

among PHLE cells derived from lung tissue of different donor organs, but this variation was similar to Hep-2 cell replicates. CX3CR1 protein levels were also readily detected in PHLE cultures from multiple donors and were nearly twofold higher in PHLE cells compared to Hep-2 cells (Fig. 3b). Taken together, CX3CR1 transcript and protein was detected in ALI cultures of differentiated pediatric lung epithelial cells.

We evaluated the functional role of CX3CR1 in RSV infection of pediatric lung epithelial cells. PHLE cells were differentiated at ALI as described and challenged at the apical surface with RSV engineered to express GFP.<sup>6</sup> PHLE cell cultures were readily infected, as defined by detection of GFP fluorescence in <24 h,

and lasting for >72 h, following challenge (Fig. 4a, data not shown). Evidence of productive RSV infection in PHLE cell cultures is demonstrated by detection of GFP foci and viral transcript (RSV-M). GFP at 24–48 h was focal and dispersed throughout the culture (Fig. 4a). Preincubation of PHLE cell cultures with anti-CX3CR1 antibody prior to RSV infection significantly decreased RSV infection as defined by the number of GFP foci detected (Fig. 4a, b). Using flow cytometry, we found a significant increase in the GFP intensity in PHLE cell cultures expressing CX3CR1, compared to CX3CR1-negative cells following RSV infection (Fig. 3c). We also found a dose-dependent reduction in the levels of viral transcript production following treatment of PHLE with anti-CX3CR1 antibody (Fig. 4c). To confirm the involvement of CX3CR1 in PHLE cell culture infection by RSV, we incubated the virus with recombinant CX3CR1 (rCX3CR1) prior to infection. We found a significant reduction in RSV-M transcript and FFUs after preincubation with rCX3CR1 (Fig. 4d, e). Taken together, these results support that CX3CR1 is expressed in pediatric lung epithelial cells and serves a functional role during infection by RSV. Furthermore, this suggests that CX3CR1-expressing cells are highly susceptible to RSV infection.

### DISCUSSION

In this report, we show that CX3CR1 mRNA is expressed in airway epithelial cells from the pediatric respiratory tract, including nasal epithelial cells from 53 asymptomatic healthy 1-month-old infants and multiple cell types from 11 pediatric lung tissues. Expression appears to be more common in the upper airway than in the lower airway but is not always detectable in either location. In vivo, we present evidence that CX3CR1 expression occurs in cells that appear to be ciliated in agreement with other reports using adult cells,<sup>17</sup> in addition to other cells not displaying the ciliated cell marker. Using a lung epithelial cell in vitro model derived from primary pediatric epithelial cells, we demonstrated that RSV viral loads are the highest in cells expressing CX3CR1 and that blocking CX3CR1–RSV interaction significantly reduces the levels of RSV infection. Taken together, our results support the expression of CX3CR1 in the airways of children, where it can contribute to productive RSV infection in the airways.

Perhaps, the most surprising finding of our study is the low, and often undetected, RNA expression of CX3CR1 transcript in pediatric lung epithelial cells. Although expression is readily found in other cells in the lung, such as immune cells, epithelial cells appear to express lower levels of CX3CR1 mRNA. Despite this, CX3CR1 protein was detected in the lung epithelium of all subjects we examined. These results are consistent with other reports showing the expression of CX3CR1 in normal human bronchial epithelial cell models.<sup>14,15</sup>

We used a novel, physiological model of pediatric lung epithelium. We found that CX3CR1 RNA and protein was expressed in our pediatric model of lung epithelium. The higher levels of CX3CR1 in PHLE cell cultures compared to commonly

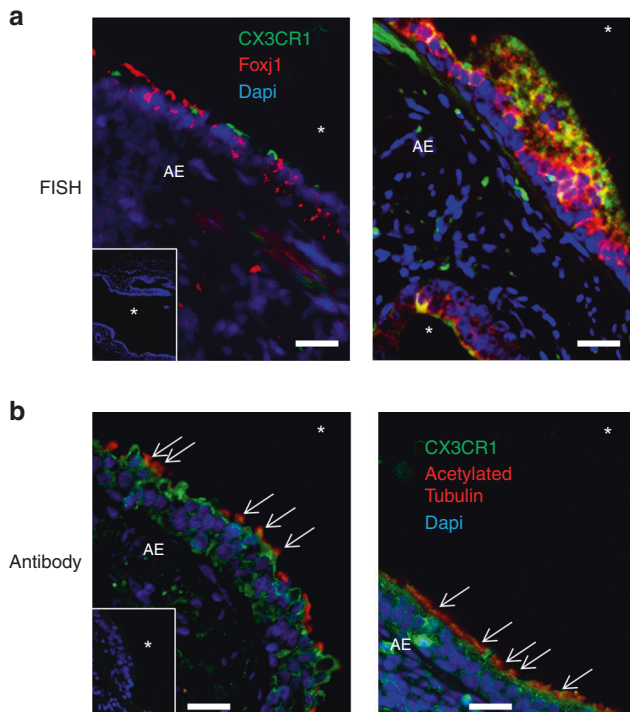


**Fig. 2** CX3CR1 expression in the pediatric airways. **a** FISH of pediatric lung samples probed for CX3CR1 (green), Foxj1 (red), and nuclei (blue) for two subjects. In-laid image: negative probe straining for green and red probes and stained for nuclei (blue). Representative images from tissue from two out of three subjects with two slides per subject performed in duplicate. **b** Lung specimens probed with anti-CX3CR1 antibody (green), anti-acetylated tubulin antibody (red), and counterstained with Dapi nuclear stain (blue). Representative images from tissue from two out of four subjects with three slides per subject performed in duplicate. In-laid image: negative control probed with unimmunized rabbit IgG (green) or mouse IgG (red) and counterstained with nuclear stain (blue). Arrows indicate regions of CX3CR1/acetylated tubulin colocalization. White asterisk (\*) denotes airway lumen.

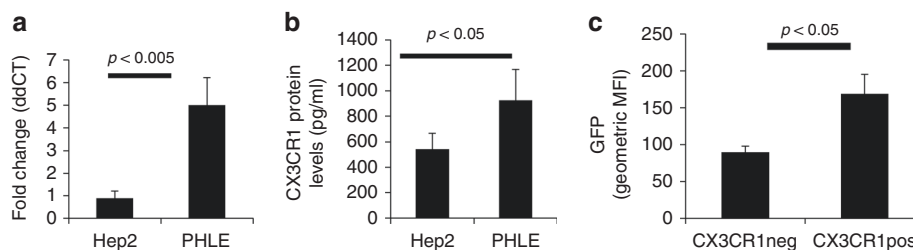


**Fig. 3** Role of CX3CR1 in RSV infection of pediatric epithelial cells. **a** RNA transcript levels of PHLE cell cultures 14 days post-ALI ( $N = 4$ ) measured by quantitative PCR for the CX3CR1 transcript. Hep-2 cell line ( $N = 3$ ) was used for comparison. **b** Protein levels of PHLE cell cultures 14 days post-ALI ( $N = 4$ ) measured by sandwich ELISA from cell protein lysates. Hep-2 cell line ( $N = 3$ ) was used for comparison. **c** Flow cytometric analysis of CX3CR1-positive and -negative cells after infection of PHLE cell cultures for 48 h and with GFP-expressing RSV ( $N = 3$ ).

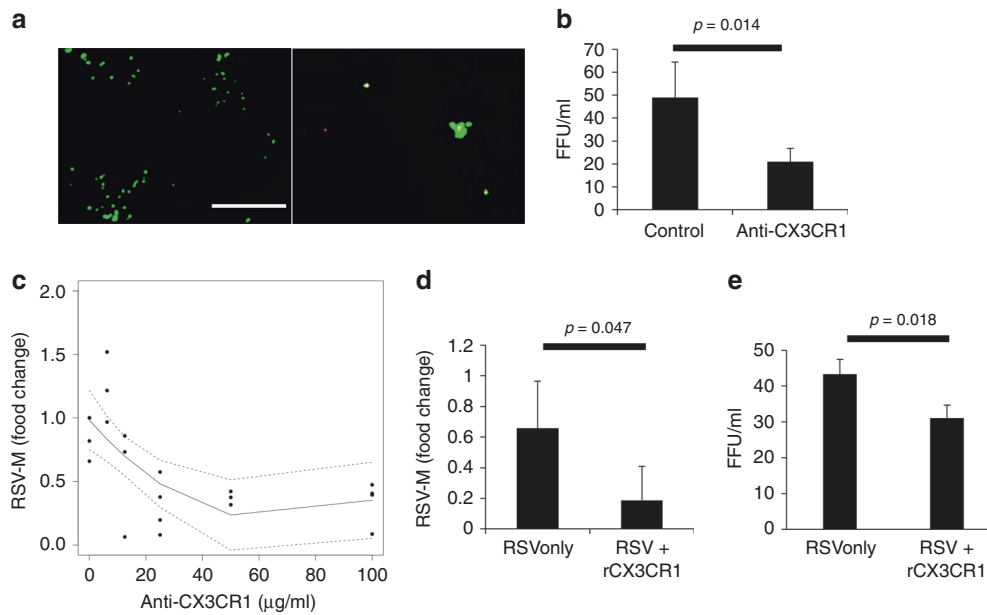


**Fig. 4** Effect of blocking CX3CR1 on RSV infection. **a** Representative fluorescent images of 24 h postinfection PHLE cell cultures infected with GFP-expressing RSV virus after cells were incubated for 30 min with (left) control antibody or (right) anti-CX3CR1 antibody. **b** Average RSV fluorescent focus-forming units per ml detected 24 h postinfection with or without CX3CR1-blocking antibody (25  $\mu$ g/ml) ( $N = 4$ ). **c** Dose–response curve of RSV quantification by qPCR of PHLE cell cultures infected with RSV after preincubation with varying levels of anti-CX3CR1 antibody ( $N = 4$ ). **d** RSV M-protein transcript levels or **e** fluorescent foci 24 h postinfection with or without preincubation of RSV with recombinant CX3CR1 protein ( $N = 4$ ).

used cell line, HEp-2, demonstrates the importance of using the correct model to study RSV infection. Upon infection, RSV transcript levels were the greatest in PHLE cells expressing CX3CR1. Although we did not discriminate primary vs secondary infection in our model, the increase in RSV transcript levels in CX3CR1-expressing cells supports that RSV preferentially targets CX3CR1-expressing cells. Both CX3CR1-blocking antibody and recombinant proteins significantly reduce RSV load, although we cannot discern the effect of CX3CL1 in our assays. Other studies using adult epithelial cells have demonstrated similar findings.<sup>14,15</sup>

Our results do not demonstrate that CX3CR1 is necessary for RSV infection but contributes to maximal productive infection. Even with high concentrations of blocking antibody, RSV infection was still established. This is consistent with reports showing that RSV viruses lacking the G protein can still replicate in vitro,<sup>24</sup> although it is worth noting that these viruses do not cause disease in mice.<sup>24</sup> In addition, publicly available results from the Lung Molecular Atlas Program profiling project (LungMAP) show expression of heparan sulfate-containing proteins (Syndecans) and Nucleolin in lung epithelium.<sup>22</sup> Although expression of heparan sulfate-containing proteins in the airways is still debated,<sup>25</sup> our results suggest the presence of at least two receptors capable of mediating productive RSV infections. Given the known binding of RSV to heparin, heparan sulfate, and chondroitin sulfate-containing proteins<sup>1</sup> as well as Nucleolin,<sup>2</sup> future studies are needed to further examine their role in RSV infection of PHLE. Furthermore, we did not discern the role CX3CL1 plays in these infections and what part disruption of CX3CL1/CX3CR1 ligand–receptor pathway by RSV plays in this reduction of viral load is still largely unknown.

It should not be overlooked that the expression of CX3CR1 in the lung was not restricted to epithelial cells but rather that many cell types express CX3CR1 (Fig. 1c). We found high RNA expression levels of CX3CR1 in immune cells derived from the lung. Although we did not probe for immune cell markers during histological analysis of pediatric lung tissue, we found rounded cells,

presumable immune cells, expressing CX3CR1. Given the presence of alveolar macrophages<sup>26</sup> and T cells<sup>27</sup> on the apical surface of lung epithelium and the ability of RSV to infect a multiplicity of cells, including CX3CR1-expressing immune cells,<sup>28</sup> it is possible that immune cells play a role in RSV replication.<sup>29,30</sup> In addition, severe cases of RSV have demonstrated increases of immune cells in the lung.<sup>31</sup> Taken together, further studies are needed to understand the role of CX3CR1 expression on lung-infiltrating immune cells and what role this plays in RSV infection and disease severity.

Although there is now considerable evidence that CX3CR1 plays a role as receptor in RSV infection, RSV infection of lung epithelium is more complex than modeled here. Animal models are needed to fully understand the consequence of CX3CR1 expression in cells in the lung. In addition, our assay did not directly measure attachment of RSV to the lung epithelium via CX3CR1, therefore future studies will be needed to determine the specific role CX3CR1 plays in the airways. Furthermore, transcript levels were low and often undetectable in the epithelial cells of the lung, yet we suggest that sufficient levels of CX3CR1 protein exist despite the low transcript levels. There are no data to suggest that differences in CX3CR1 expression among individuals contributes to the likelihood or severity of infection, but this should be assessed more thoroughly. Overall, our work suggests CX3CR1 as a therapeutic target and supports studies aimed at blocking G protein/host–epithelial interaction as a means to limit RSV infection in children.

#### ACKNOWLEDGEMENTS

This work was supported by the University of Rochester Respiratory Pathogen Research Center NIH/NIAID, HHSN272201200005C, the LungMAP Consortium including 1U01HL122700, and the University of Rochester Pulmonary training grant T32-HL066988. We greatly appreciate the donor tissue, precious gifts generously given, supplied through the US DHHS Donation and Transplantation Network and the organizations that link donor families to the scientific community.

## AUTHOR CONTRIBUTIONS

Each author has met the *Pediatric Research* authorship requirements. C.S.A., E.E.W. and T.J.M. conceptualized the study. C.S.A., T.J.M., C.Y.-C., Q.W., E.E.W., J.A.M., Y.R. and G.S.P. designed the experiments. T.J.M., G.S.P. and R.M. developed the cohort and collected the specimens. C.S.A., K.D., T.J.M., C.Y.-C., J.M., Y.R. and S.B. generated, analyzed and interpreted the data. C.S.A., C.Y.-C., J.A.M., G.S.P., E.E.W. and T.J.M. wrote and/or revised the manuscript.

## ADDITIONAL INFORMATION

**Competing interests:** The authors declare no competing interests.

**Publisher's note** Springer Nature remains neutral with regard to jurisdictional claims in published maps and institutional affiliations.

## REFERENCES

- Hallak, L. K., Collins, P. L. & Knudson, W. Iduronic acid-containing glycosaminoglycans on target cells are required for efficient respiratory syncytial virus infection. *Virology* **271**, 264–275 (2000).
- Tayyari, F. et al. Identification of nucleolin as a cellular receptor for human respiratory syncytial virus. *Nat. Med.* **17**, 1132–1135 (2011).
- Hallak, L. K., Kwilas, S. A. & Peeples, M. E. Interaction between respiratory syncytial virus and glycosaminoglycans, including heparan sulfate. *Methods Mol. Biol.* **379** (Chapter 2), 15–34 (2007).
- Sigurs, N. et al. Severe respiratory syncytial virus bronchiolitis in infancy and asthma and allergy at age 13. *Am. J. Respir. Crit. Care Med.* **171**, 137–141 (2005).
- Fields, B. N. *Fields Virology* (Stanford University Press, 2013).
- Hallak, L. K., Spillmann, D., Collins, P. L. & Peeples, M. E. Glycosaminoglycan sulfation requirements for respiratory syncytial virus infection. *J. Virol.* **74**, 10508–10513 (2000).
- Zhang, H. et al. Differential expression of syndecan-1 mediates cationic nanoparticle toxicity in undifferentiated versus differentiated normal human bronchial epithelial cells. *ACS Nano* **5**, 2756–2769 (2011).
- Lee, M., Lee, Y., Song, J., Lee, J. & Chang, S.-Y. Tissue-specific role of CX3CR1 expressing immune cells and their relationships with human disease. *Immune Netw.* **18**, e5 (2018).
- Liang, B. et al. Effects of alterations to the CX3C motif and secreted form of human respiratory syncytial virus (RSV) G protein on immune responses to a parainfluenza virus vector expressing the RSV G protein. *J. Virol.* **93**, e02043 (2019).
- Tripp, R. A. et al. CX3C chemokine mimicry by respiratory syncytial virus G glycoprotein. *Nat. Immunol.* **2**, 732–738 (2001).
- Jones, H. G. et al. Structural basis for recognition of the central conserved region of RSV G by neutralizing human antibodies. *PLoS Pathog.* **14**, e1006935 (2018).
- McLellan, J. S., Ray, W. C. & Peeples, M. E. Structure and function of respiratory syncytial virus surface glycoproteins. *Curr. Top. Microbiol. Immunol.* **372**, 83–104 (2013).
- Fedechkin, S. O., George, N. L., Wolff, J. T., Kauvar, L. M. & DuBois, R. M. Structures of respiratory syncytial virus G antigen bound to broadly neutralizing antibodies. *Sci. Immunol.* **3**, eaar3534 (2018).
- Johnson, S. M. et al. Respiratory syncytial virus uses CX3CR1 as a receptor on primary human airway epithelial cultures. *PLoS Pathog.* **11**(Dec), e1005318 (2015).
- Chirkova, T. et al. CX3CR1 is an important surface molecule for respiratory syncytial virus infection in human airway epithelial cells. *J. Gen. Virol.* **96**(Sep), 2543–2556 (2015).
- Liesman, R. M. et al. RSV-encoded NS2 promotes epithelial cell shedding and distal airway obstruction. *J. Clin. Invest.* **124**, 2219–2233 (2014).
- Jeong, K.-I. et al. CX3CR1 is expressed in differentiated human ciliated airway cells and co-localizes with respiratory syncytial virus on cilia in a G protein-dependent manner. *PLoS ONE* **10**, e0130517 (2015).
- Choi, Y., Mason, C. S., Jones, L. P. & Viral, J. C. 2012. Antibodies to the central conserved region of respiratory syncytial virus (RSV) G protein block RSV G protein CX3C-CX3CR1 binding and cross-neutralize RSV A and B strains. *Viral Immunol.* **25**(Jun), 193–203 (2012).
- Boyoglu-Barnum, S. et al. An anti-G protein monoclonal antibody treats RSV disease more effectively than an anti-F monoclonal antibody in BALB/c mice. *Virology* **483**, 117–125 (2015).
- Walsh, E. E., Falsey, A. R. & Sullender, W. M. Monoclonal antibody neutralization escape mutants of respiratory syncytial virus with unique alterations in the attachment (G) protein. *J. Gen. Virol.* **79**(Pt 3), 479–487 (1998).
- Wang, Q. et al. A novel in vitro model of primary human pediatric lung epithelial cells. *Pediatr. Res.* **41**, 2294 (2019).
- Bandyopadhyay, G. et al. Dissociation, cellular isolation, and initial molecular characterization of neonatal and pediatric human lung tissues. *Am. J. Physiol. Lung Cell. Mol. Physiol.* **315**, L576–L583 (2018).
- Chu, C.-Y. et al. The healthy infant nasal transcriptome: a benchmark study. *Sci. Rep.* **6**, 33994 (2016).
- Karron, R. A. et al. Respiratory syncytial virus (RSV) SH and G proteins are not essential for viral replication in vitro: clinical evaluation and molecular characterization of a cold-passaged, attenuated RSV subgroup B mutant. *Proc. Natl Acad. Sci.* **94**, 13961–13966 (1997).
- Zhang, L., Peeples, M. E., Boucher, R. C., Collins, P. L. & Pickles, R. J. Respiratory syncytial virus infection of human airway epithelial cells is polarized, specific to ciliated cells, and without obvious cytopathology. *J. Virol.* **76**, 5654–5666 (2002).
- Hussell, T. & Bell, T. J. Alveolar macrophages: plasticity in a tissue-specific context. *Nat. Rev. Immunol.* **14**, 81–93 (2014).
- Holtzman, M. J. et al. Immunity, inflammation, and remodeling in the airway epithelial barrier: epithelial-viral-allergic paradigm. *Physiol. Rev.* **82**, 19–46 (2002).
- Raiden, S. et al. Respiratory syncytial virus (RSV) infects CD4+ T cells: frequency of circulating CD4+ RSV+ T cells as a marker of disease severity in young children. *J. Infect. Dis.* **215**, 1049–1058 (2017).
- Zhivaki, D. et al. Respiratory syncytial virus infects regulatory B cells in human neonates via chemokine receptor CX3CR1 and promotes lung disease severity. *Immunity* **46**, 301–314 (2017).
- Cirino, N. M. et al. Restricted replication of respiratory syncytial virus in human alveolar macrophages. *J. Gen. Virol.* **74**(Pt 8), 1527–1537 (1993).
- Openshaw, P. J. M. & Tregoning, J. S. Immune responses and disease enhancement during respiratory syncytial virus infection. *Clin. Microbiol. Rev.* **18**, 541–555 (2005).